Macromolecules

pubs.acs.org/Macromolecules

Article

Ion Specificity Influences on the Structure of Zwitterionic Brushes

Qiming He,* Yijun Qiao, Carlos Medina Jimenez, Ryan Hackler, Alex B. F. Martinson, Wei Chen,* and Matthew V. Tirrell*

Cite This: *Macromolecules* 2023, 56, 1945−1953

Read Online

ACCESS | Metrics & More | Article Recommendations | Supporting Information

ABSTRACT: Zwitterionic brushes have a wide range of applications, including use as lubricating surfaces and antifouling membranes. In this study, densely end-tethered poly(cysteine methacrylate) (PCysMA) brushes were synthesized using surface-initiated activators regenerated by electron transfer atom transfer radical polymerization (SI-ARGET-ATRP). The structure of the PCysMA brushes was investigated using ellipsometry, X-ray reflectivity (XRR), attenuated total reflection Fourier transform infrared spectroscopy (ATR-FTIR), and atomic force microscopy (AFM). The results of these characterization techniques were used to study the effect of SO_4^{2-}, Cl^-, NO_3^-, Br^-, and SCN^- anions, divalent Ca^{2+} and Ba^{2+} cations, and trivalent Y^{3+} cations on the structure of the PCysMA brushes. The results showed that the PCysMA brushes in solution exhibit an "antipolyelectrolyte" effect to a certain degree, which inversely follows the Hofmeister series of anions. The introduction of divalent cations Ca^{2+} and Ba^{2+} had a modest impact on the dimensions of the PCysMA brushes, indicating that chelating interactions between the cations and zwitterion units work against the "antipolyelectrolyte" effect. The complexation was even stronger in the presence of trivalent Y^{3+} cations, which caused the PCysMA brushes to shrink. These findings highlight the importance of ion specificity to the structure of zwitterionic brushes in aqueous solutions.

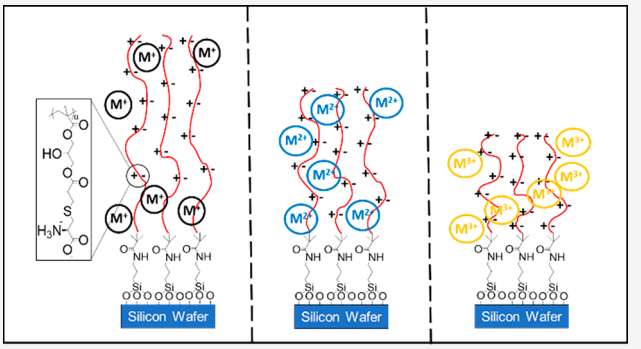

INTRODUCTION

Nonspecific adsorption of biomacromolecules and microorganisms on surfaces poses great challenges in many applications, ranging from biomedical sensors to ship hulls.[1,2] To address these challenges, zwitterionic polymeric materials have been proved to be a promising and effective candidate. Zwitterionic polymers, or polyzwitterions, encompass a group of ampholytic polymers, bearing pairs of cationic and anionic side groups while remaining net-neutrally charged.[3,4] Due to their well-hydrated structures,[5,6] zwitterionic polymers are resistant to nonspecific protein adsorption, cell adhesion, and subsequent biofilm formation, explaining why they have been widely investigated as nontoxic antifouling materials for biomedical and engineering materials.[7−11]

In practice, there are only a few materials used for the aforementioned purposes. Poly(ethylene glycol) (PEG)-based materials have been widely used for their high resistance toward nonspecific protein adsorption and cell adhesion.[12] However, PEG materials are subject to long-term degradation, as these can be oxidized under an open-air atmosphere and lose function in biological media.[13] Resistance to nonspecific adsorption and cell adhesion is generally attributed to the strong hydration of PEG chains,[14] which has been examined by computer simulations using oligo(ethylene glycol) self-assembled monolayers (SAM) as model systems.[15,16] These studies revealed the presence of a tightly bound water layer around the SAM, which leads to repulsive forces that prevent protein adsorption on these surfaces.[15,16] While hydration layers in PEG-based materials are primarily formed through hydrogen bonding, zwitterionic materials are presumably able to bind water molecules more strongly through electrostatically induced hydration,[5,6] often conferring on the latter better capabilities at nonspecific protein adsorption and cell adhesion.[17]

In contrast to typical polyelectrolyte brushes, which stretch in pure water but shrink in salt solutions,[18] some zwitterionic brushes adopt a behavior of stretching in salt solutions yet shrinking in pure water, dubbed the "antipolyelectrolyte" effect. This phenomenon is caused by the balance between ion-pairing interactions, dipole orientations, and local dielectric constants within brushes, which screen the attractive interactions between positive and negative charges within the zwitterionic units.[6]

Despite significant advancements in the development of zwitterionic brushes, in both academic and industrial settings, a

Received: October 1, 2022
Revised: January 15, 2023
Published: February 24, 2023

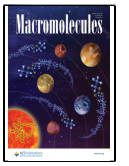

Scheme 1. (a) Surface Cleaning and Initiator Immobilization on Silicon Substrates, (b) Synthesis of the CysMA Monomer, and (c) Synthesis of a PCysMA Brush via ARGET-ATRP

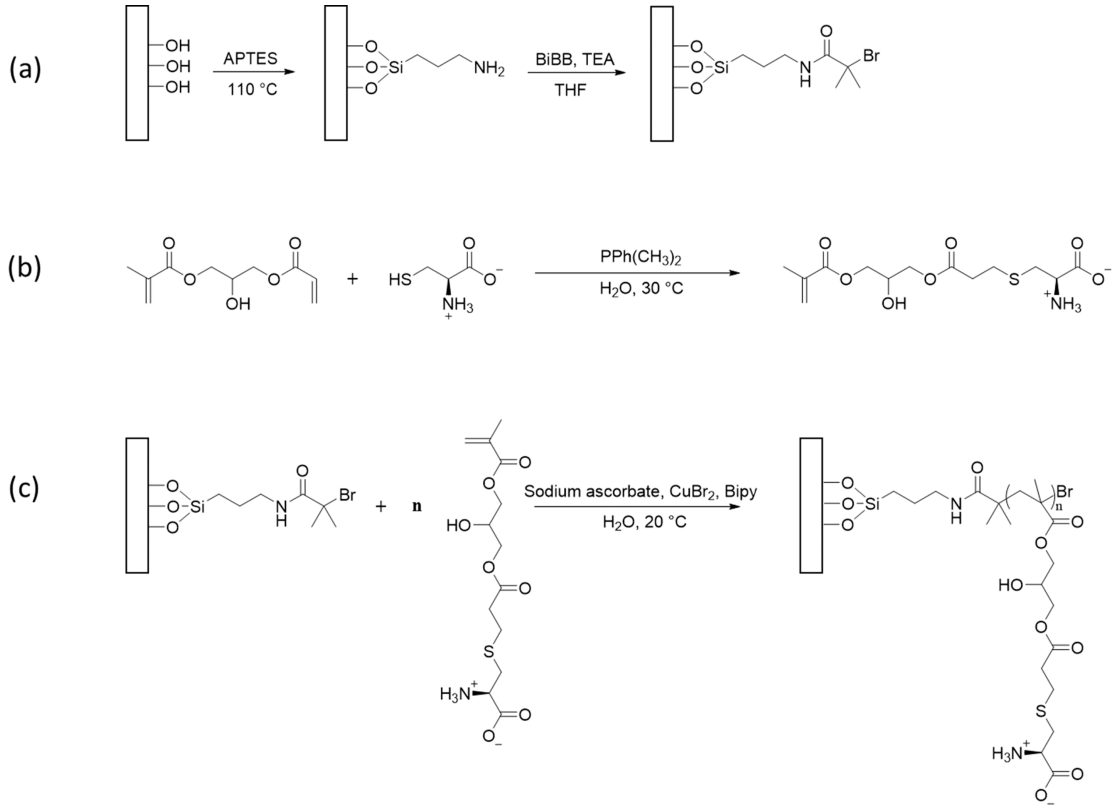

more comprehensive understanding on the effect of salt addition on the structure of zwitterionic brushes, specifically those bearing amino acid motifs as side chains, is needed. In particular, the formation of different types of conjugate structures between salt ions and zwitterionic moieties is expected to produce a significant impact on macromolecular architectures within the brushes. The extent of the formation of ion−brush complexes, which include monodentate, bridging bidentate, and chelating bidentate coordination, can be dictated by the ionic strength, which in turn can be exploited to tune the brush properties at the nanoscale.

To address this issue, a densely tethered zwitterionic polymer brush containing amino acid moieties, poly(cysteine methacrylate) (PCysMA), with a fairly narrow distribution of chain length, was synthesized via SI-ATRP.[19] The properties of PCysMA brushes were thoroughly investigated in the presence of salts of different identities with two main purposes: (I) To investigate the association of anions with zwitterionic groups, various anions were selected from the Hofmeister series, which ranks ions according to their ability at precipitating proteins[20] and will allow for a systematic understanding of how to tune interactions between anions and amino acid groups.[21] (II) To study the effect of multivalent cations interacting with carboxylate groups, three ionic compounds, $Ca(NO_3)_2$, $Ba(NO_3)_2$, and $Y(NO_3)_3$, were employed. A combination of attenuated total reflection Fourier transform infrared spectroscopy (ATR-FTIR), X-ray reflectometry (XRR), ellipsometry equipped with a liquid cell, and atomic force microscopy (AFM) was used in concert to reveal the intriguing structures of PCysMA brushes in these various conditions.

EXPERIMENTAL SECTION

Materials. (3-Aminopropyl)triethoxysilane (APTES, 99%), α-bromoisobutyryl bromide (BIBB, 98%), triethylamine (TEA, ≥99%), 2,2′-bipyridine (bpy, >99%), 3-(acryloyloxy)-2-hydroxypropyl methacrylate (99%), L-cysteine (97%), sodium L-ascorbate (≥99.0%), dimethylphenylphosphine (DMPP, 99%), copper(II) bromide (Cu(II)Br, >99%), sodium thiocyanate (NaSCN, ≥99.99% trace metals basis), sodium bromide (NaBr, ≥99.99% trace metals basis), sodium chloride (NaCl, ACS reagent, ≥99.0%), sodium nitrite ($NaNO_3$, ACS reagent, ≥99.0%), sodium sulfate (Na_2SO_4, ACS reagent, ≥99.0%, anhydrous, powder), calcium nitrate tetrahydrate ($Ca(NO_3)_2{\cdot}4H_2O$, ACS reagent, 99.0%), barium nitrate ($Ca(NO_3)_2$, 99.999% trace metals basis), yttrium(III) nitrate tetrahydrate, ($Y(NO_3)_3{\cdot}4H_2O$, 99.999% trace metals basis), tetrahydrofuran (THF, anhydrous, 99.8%), dichloromethane (DCM, ACS reagent, ≥99.5%, containing 40−150 ppm amylene as stabilizer), ethyl acetate (ACS reagent, ≥99.5%), methanol (≥99.9%), and deuterium oxide (D_2O, 99.9 atom % D) were purchased from Sigma-Aldrich. 3-(acryloyloxy)-2-hydroxypropyl methacrylate was purified with inhibitor removers (Sigma-Aldrich) before thia-Michael addition, and the other chemicals were used without further purification. Single side polished silicon wafers ([100] orientation, 4 in. diameter, 500 μm thickness) were purchased from University Wafer (Boston, MA). Deionized water was prepared from a Millipore Milli-Q system with a resistivity of 18.2 MΩ·cm.

Surface Cleaning and Initiator Immobilization. Silicon wafers were pieced into 10 mm × 55 mm rectangles and then cleaned with a Nano-Strip (KMG Chemicals) solution. A layer of APTES was first deposited onto the silicon substrates via vapor deposition (0.015 mbar) in a vacuum chamber for 1 h, followed by annealing at 110 °C in air for 1 h. An ATRP initiator, BIBB (0.94 mL, 8.40 mmol), was grafted to the APTES monolayer in THF (40 mL) with triethylamine (1.20 mL, 8.40 mmol), as illustrated in Scheme 1a.

Preparation of Cysteine Methacrylate (CysMA). The synthesis of the CysMA monomer was based on the protocols by Armes and

https://doi.org/10.1021/acs.macromol.2c02029
Macromolecules 2023, 56, 1945−1953

co-workers.[19] L-Cysteine (22.00 g, 181.57 mmol) was dissolved in deionized water (120 mL), and the solution was deoxygenated by nitrogen purging for 30 min. DMPP (30 μL, 221 μmol) and 3-(acryloyloxy)-2-hydroxypropyl methacrylate (40.57 g, 189.37 mmol) were added to cysteine solution under the protection of nitrogen, and the aqueous solution was stirred at ambient temperature for 2 h, as shown in Scheme 1b The reaction solution was then purified twice with DCM (80 mL) and ethyl acetate (80 mL). CysMA monomer was isolated and dried using a lyophilizer and characterized using ^{1}H NMR.

Synthesis of PCysMA Brushes. PCysMA brushes were prepared by Activators Regenerated by Electron Transfer (ARGET-ATRP),[22] as shown in Scheme 1c. In a typical reaction, CysMA (20.0 g, 60.0 mmol), bpy (51.5 mg, 0.33 mmol), and Cu(II)Br_2 (7.4 mg, 0.033 mmol) were dissolved in deionized water (45.0 mL). After deoxygenation by nitrogen purging for 30 min, sodium L-ascorbate (65.3 mg, 0.33 mmol) was added to the aqueous solution under nitrogen flow. The solution was then syringed over the substrates in a vacuum chamber, and the polymerization was allowed to proceed at ambient temperature. After the desired reaction time, the polymerization was terminated by exposing the solution to air. The samples were then rinsed with water and dried under a stream of nitrogen gas.

X-ray Reflectivity (XRR). XRR measurements were performed at the Advanced Photon Source (APS) beamline 33-BM-C with a liquid cell. An X-ray energy of 21 keV was used with a beam size of 900 μm × 500 μm and a charge coupled device 2D detector. A vertical resolution of 17.9 Å was achieved using the setup at the beamline. PCysMA brushes were immersed in aqueous solutions for 15 min before XRR data were collected. A four-layer model was developed to analyze data from a system consisting of a Si/SiO_x/brush layer/aqueous layer, where the thickness of the SiO_x layer and the roughness of the Si/SiO_x interface were fixed among the substrates, which were 18.9 and 4.5 Å by value, respectively. The components and concentration of the aqueous solutions were known. Thus, the SLD values of aqueous solution were calculated theoretically, which are listed in Table S1. In the model, the root-mean-square roughness was used to describe the rough interface.[23] The interface was expressed by an ensemble of smooth interface with certain z-coordinates $z_j + z$, weighted by a probability density $P_j(z)$ with mean value

$$\mu_j = \int zP_j(z)\,\mathrm{d}z$$

and root-mean-square roughness

$$\sigma_j^2 = \int (z-\mu_j)^2 P_j(z)\,\mathrm{d}z$$

Ellipsometry. The dry thickness of PCysMA brushes on a Si wafer was modeled using an Alpha-SE spectroscopic ellipsometer (J. A. Woollam Co., Lincoln, NE) at multiple incident angles of 65°, 70°, and 75°. The ellipsometric data were fit to a three-layer model (Si/SiO_x/brush layer), in which optical constants of the Si and native SiO_x (fixed to 1.49 nm) were taken from CompleteEASE software's library database. A transparent Cauchy model, $n(\lambda) = A + B/\lambda^2$, was used to model the brush layer for which A and B were fitted as 1.502 and 0.012 μm^2, respectively. Measurements of brushes immersed in aqueous solutions were conducted using an Alpha-SE 500 μm liquid cell with fused silica windows (J. A. Woollam Co., Lincoln, NE) at an incident angle of 70°. The resultant data were analyzed with window corrections using a four-layer model (Si/SiO_x/brush layer/aqueous layer) with fixed optical values for Si, native SiO_x (fixed at 1.49 nm), and water from CompleteEASE software's library database. The thickness and refractive index of the brush layer were fitted using a Cauchy layer, $n(\lambda) = A + B/\lambda^2$, where A varied from 1.445 to 1.486 and B was around 0.020 μm^2. Three measurements were conducted for each condition such that a mean and standard deviation could be derived.

Atomic Force Microscopy (AFM). Height and phase images of PCysMA brushes in aqueous solutions were acquired using a MFP3D-SA AFM (Asylum Research, Oxford Instruments, Goleta, CA) in Tapping mode. AFM probes (qp-HBC, Nanosensors, Neuchatel, Switzerland) with nominal force constants of 0.35−0.8 N/m and typical tip radius of curvature smaller than 10 nm were used. Prior to the measurements, each substrate was immersed in the aqueous solution for 15 min.

Attenuated Total Reflection Fourier Transform Infrared (ATR-FTIR) Spectroscopy. ATR-FTIR measurements were performed using an Alpha II FTIR spectrometer (Bruker) with a Diamond Crystal ATR accessory. Substrates were immersed in various aqueous solutions (D_2O used as solvent) for 15 min before each measurement. ATR-FTIR spectra were acquired between 400 and 4000 cm^{-1}.

Nuclear Magnetic Resonance (NMR). ^{1}H solution NMR spectra were obtained on a 500 UltraShield Plus spectrometer (Bruker, 500 MHz) using approximately 30 mg of sample dissolved in 1 mL of deuterium oxide.

RESULTS AND DISCUSSION

PCysMA brushes were synthesized via SI-ARGET-ATRP of CysMA monomers.[22] Armes and co-workers have demonstrated a facile and robust route to synthesize high purity CysMA monomers.[19,24] However, the thickness of zwitterionic brushes produced using CysMA under conventional SI-ATRP conditions was limited to about 27 nm,[19] which hampers the ATR-FTIR characterization of the brushes. To overcome the thickness limitation, ARGET-ATRP, in which ATRP activators were regenerated by reducing agents, was used prepare the PCysMA brushes.[22] Using this strategy, PCysMA brushes with a larger thickness of 97 ± 2 nm in the dry state were achieved. While experience shows that surface-initiated ATRP produces a fairly narrow distribution of chain lengths, there is no reliable method to determine the molecular weight of end-tethered chains. The results we report here, which concern comparative local ion binding at fixed grafting density, should not depend significantly on chain length. Assuming the grafting density to be 0.1 chain/nm^2, a brush with thickness of 97 nm corresponds to a number-average molecular weight of the grafted polymer chains of 584 kg/mol. It may be interesting to explore effects of grating density in future work.

In its natural form, L-cysteine is pH-responsive, with an isoelectric point at pH of 5.02,[25] resulting in the environmental dependence of the PCysMA brushes in aqueous solutions. These weak zwitterionic brushes may differ significantly as a function of pH from permanently zwitterionic betaine-based brushes. However, through ellipsometry, AFM, and surface zeta potential characterizations, Armes and co-workers were able to experimentally determine the zwitterionic regime of PCysMA to be between pH 2.0 and pH 9.5.[19] The pH values of the aqueous solutions used in this study all fell within the zwitterionic regime, as detailed in Table S2.

Brush Dimension Follows Inverse Hofmeister Series. The first set of salts used in this work include SO_4^{2-} > Cl^- > Br^- > NO_3^- > SCN^-, ordered by decreasing ability at protein precipitation,[20] correlated to the chaotropic character of the anions.[21] Schlenoff and co-workers studied the anion-specific interactions with a zwitterionic polymer, poly(sulfobetaine acrylamide), through hydrodynamic radius (R_h) measurements using a set of anions located along the Hofmeister series, and found a strong correlation between the R_h of the polymer chains and the chaotropic character of the anions in aqueous solutions, in which the maximum R_h was observed with the most chaotropic anion, SCN^-.[26]

The effect of anions on PCysMA brush dimensions as a function of concentration was investigated using ellipsometry,

https://doi.org/10.1021/acs.macromol.2c02029
Macromolecules 2023, 56, 1945−1953

as shown in Figure 1. The mean brush thickness in most salt solutions (NaCl, $NaNO_3$, NaBr, and NaSCN) was invariant at

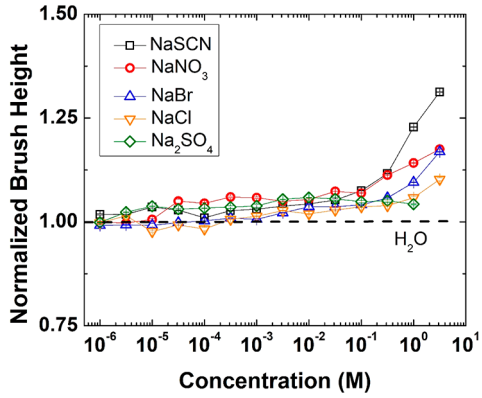

Figure 1. Brush height measured by ellipsometry plotted against the concentration of anions follow Hofmeister series: SO_4^{2-}, Cl^-, NO_3^-, Br^-, and SCN^-.

low salt concentrations, up to 0.1 M, and then increased monotonically with the salt concentration until 3.0 M. This trend can be rationalized through the concept of *osmotic* and *salted* brush regime, which was first employed to explain the effect of salt on polyelectrolyte brushes.[18] At low salt concentration, inter-/intrachain binding of the zwitterion units forms a network of PCysMA brushes, which resist the penetration of added ions into the brush layer. At high salt concentration, ions screen the interactions between zwitterion moieties, and the "antipolyelectrolyte" effect dominates. While most salts triggered an "antipolyelectrolyte" response from the PCysMA brushes, the brush thickness remained invariant in Na_2SO_4 solutions, even after the ionic strength of Na_2SO_4 exceeded 3.0 M. The observed brush thickness behavior with most salt solutions falls in agreement with other studies, in which the studied polybetaines exhibit the same "antipolyelectrolyte" effect.[6,19,27] Among the salts investigated, NaSCN exerted a significant impact on swollen brush dimension, in consistence with the fact that less-hydrated chaotropic anions are more likely to promote the disassociation of PCysMA brush inter-/intrachain bonds among zwitterionic groups.[6] On the other hand, compared to the monovalent anions, the introduction of sulfate anions led to a different polymer brush thickness dependence. Most probably, the divalent and kosmotropic nature of sulfate anions negated the "antipolyelectrolyte" effect. The hydration state of PCysMA brushes was disturbed when an excess of strongly hydrated SO_4^{2-} was present, which counteracted the charge screening effect brought by the ions. These results are in line with the work by Takahara and co-workers, in which they verified the hydration-state modulation of zwitterionic brushes through the interplay with SO_4^{2-} using neutron reflectivity (NR).[6]

XRR and NR are powerful tools for probing polyelectrolyte/zwitterionic brushes on solid substrates at the subnanometer scale.[6,18,28−35] Compared to NR, XRR provides even higher resolution, and smaller samples can be measured using XRR. When the PCysMA brushes were analyzed, none of the XRR spectra showed clear interference fringes upon addition of aqueous solutions (Figures S1−S5), likely due to the relatively close SLD values between brush and solution. However, useful information can be extracted by analyzing XRR spectra under various conditions. The SLD profiles of the brushes in NaSCN, $NaNO_3$, NaCl, and Na_2SO_4 solutions were merely set by the function used to model the interface between layers, as seen in Figures S1−S5. The SLD values of PCysMA brush in 1 mM salt solutions resemble those of the brushes in Milli-Q water, indicating the inner structure of the brush is intact in the presence of low content of ions. However, as the salt concentration increases, the PCysMA brushes start exhibiting an anion dependence, which inversely follows the sequence of the Hofmeister series of anions. Compared with Milli-Q water, an approximate 75% swell ratio of the PCysMA brushes is observed in 3 M NaSCN, while on the other side of spectrum, the brush dimension hardly changes in 1 M Na_2SO_4, as illustrated in Figure 2a. One intriguing observation is the increase of interfacial width between brush and solution, correlated to the kosmotrope/chaotrope character of the anions as well as concentration, as shown in Figure 2b. On one hand, a more diffuse interface layer forms as the concentration of the most chaotropic anion, SCN^-, increases. On the other hand, the interfacial layer width remains constant even at high concentrations of the kosmotropic anion, SO_4^{2-}. It is plausible that a more diffuse layer in the NaSCN solution is induced by strong interactions between the SCN^- and the $-NH_3^+$ functional group on the brush. The weakly hydrated thiocyanate anions interact strongly with the ammonium groups due to the similar water affinities.[31,36] This strong interaction breaks the network of zwitterion pairs and leads to a more hydrated state of PCysMA, which in turn releases more

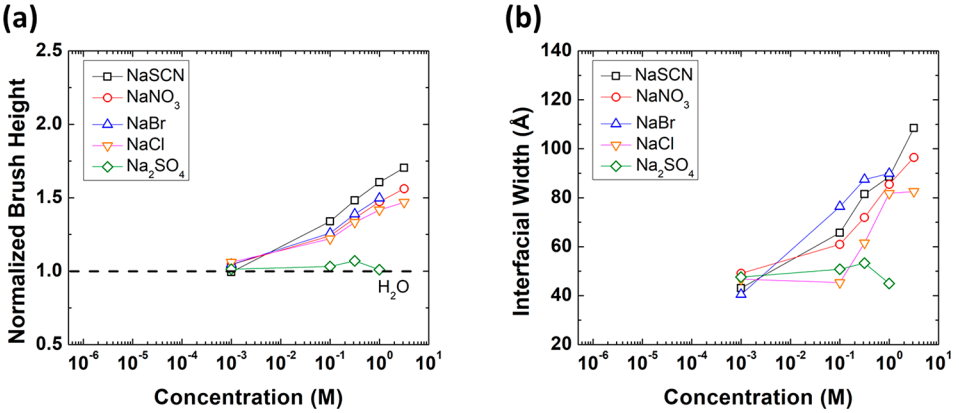

Figure 2. (a) Brush height measured by XRR plotted against the concentration of anions follow the Hofmeister series SO_4^{2-}, Cl^-, NO_3^-, Br^-, and SCN^-; (b) the corresponding interfacial width.

https://doi.org/10.1021/acs.macromol.2c02029
Macromolecules 2023, 56, 1945−1953

free brush chains into brush/solution interface. While both XRR and ellipsometry revealed the same trend upon introduction of salts, results obtained by XRR is more informative, as it surveys the sample at the subnanometer scale.

To further investigate the interfacial structure, the PCysMA brushes in aqueous solution were examined using AFM. All the AFM height images revealed a smooth brush/solution interface (Figure 3). The root-mean-square average of height deviation,

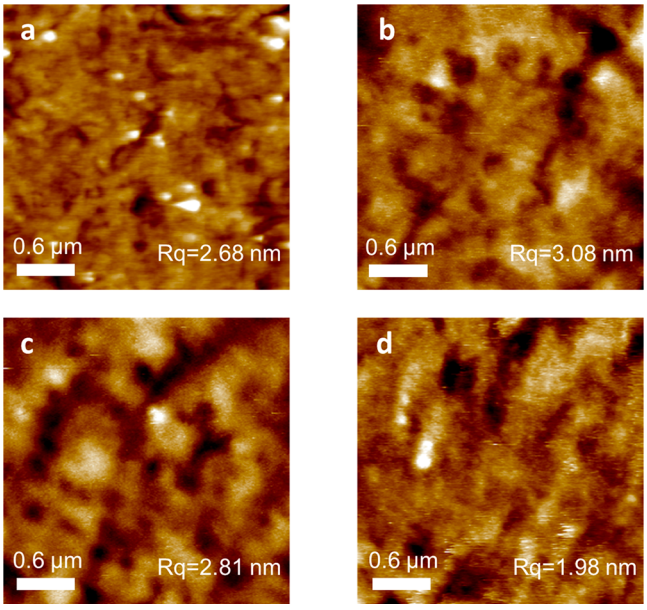

Figure 3. AFM height images of PCysMA brush in (a) Milli-Q water, (b) 3 M NaSCN, (c) 3 M $NaNO_3$, and (d) 1 M Na_2SO_4. Scan size: 3 μm × 3 μm (scale bars: 0.6 μm).

Rq, was used to characterize the interfacial width. A Rq value of 2.68 nm was obtained when the measurement was performed in Milli-Q water. When the solution was replaced with 3 M $NaNO_3$, the Rq value increased slightly to 2.81 nm, indicating the formation of a more diffuse interface. When immersed to 3 M NaSCN, an even higher Rq value of 3.08 nm was recorded. This trend corroborates the XRR results, once again demonstrating that chaotropic anions create a more diffuse brush/solution layer. Conversely, when the image was taken at 1 M Na_2SO_4, a decrease in Rq was measured, meaning the topology of PCysMA brush in the presence of a kosmotropic anion becomes more uniform as brush tails tend to be buried inside the brush layer. Similar results have been reported by Higaki, Takahara, and co-workers, in which they studied a zwitterionic brush of poly(3-(*N*-2-methacryloyloxyethyl-*N*,*N*-dimethyl)ammonatopropanesulfonate) (PMAPS) and observed a more diffuse brush/solution layer in the presence of NaSCN solutions.[31]

Complementary to the ellipsometry, XRR, and AFM results, ATR-FTIR spectra of the PCysMA brushes in solution were measured to explore further the effect of the anions on the brush structure. These ATR-FTIR spectra provide a microscopic view of the interactions between anions and amine groups in the brush at a molecular level and serve to complement the observations from XRR, ellipsometry, and AFM. Spectra were acquired using 1 M solutions of the above-mentioned salt species, as shown in Figure 4. The peak centered at 1619 cm^{-1}, correlated to the deprotonated carboxylate groups,[37,38] did not change in position upon the

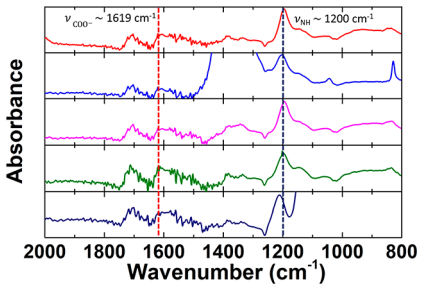

Figure 4. ATR-FTIR spectra of PCysMA brushes in 3 M NaSCN, NaBr, $NaNO_3$, NaCl, and 1 M Na_2SO_4 solutions (from top to bottom).

addition of salt (see Figure S6). This indicates a relatively weak interaction between sodium cations and brush carboxylate groups. A peak around 1200 cm^{-1} appeared when the salt solutions were introduced, which commonly corresponds to the NH bending vibration mode in amino acid groups, hinting at active interplay between the amine groups and the added ionic species.[39,40] More interestingly, a red-shift of the peak frequency by 19 cm^{-1} occurs when the SO_4^{2-} is replaced by the SCN^-.

Onsager's model provides us with one of the most straightforward routes to understanding the effect exerted by the local electrostatic fields on molecular vibrational modes. In this model, the electrostatic field exerted by the solute is treated as a dielectric continuum, and the field in turn imparts an external field to the solute.[41] The Onsager model predicts a reduction in the static dielectric constant of the solvent, which results in an observed blue-shift in the absorption peaks of vibrational probe molecules. Conversely, an increase in the solvent dielectric constant would lead to a red-shift in the absorption peaks.[41] In this study, the introduction of chaotropic anions like thiocyanate, bromide, nitrite, and chloride imparts a very different electrostatic field than that of kosmotropic anions, like sulfate. Therefore, it is likely the chaotropic nature of thiocyanate anions disturbs the hydration layers surrounding the positively charged amine moieties. Both thiocyanate and amine groups are polarizable because of their weak hydration shell,[36] so these opposite charges with a similar affinity to water form strong ion pairs between them,[42,43] creating an even higher static dielectric constant around the amine groups. On the other hand, the kosmotropic nature of sulfate anions preserves a tight hydration layer, which serves as a barrier against interaction with positively charged amine groups. The relatively loose pairs of sulfate and amine ions exert little influence on the dielectric field around the amine groups, causing a blue-shift in the C−N stretching vibration.

Effect of Divalent Cation Presence Is Ion Specific. As the brush thickness varies with salt concentration, ion specificity is another point of interest. The structural behavior of the brushes in the presence of two different divalent cations with the same anion was investigated. In contrast to the case of polyelectrolyte brushes like polystyrenesulfonate (PSS), in which the addition of divalent cations causes a dramatic decrease in the brush thickness,[18] PCysMA brushes swell slightly as a function of solution concentration, as illustrated in Figure 5. Although neither the calcium nor the barium cations have a huge impact on the dimension of PCysMA brushes, the swelling behavior of the brush is ion-specific. A subtle increase in the thickness of the brushes is observed in the $Ca(NO_3)_2$ solution up until the concentration reaches 0.1 M, after which

https://doi.org/10.1021/acs.macromol.2c02029
Macromolecules 2023, 56, 1945−1953

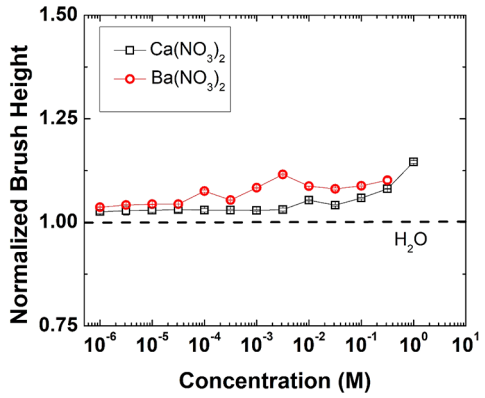

Figure 5. Brush height measured by ellipsometry plotted against the concentration of the divalent cations Ca^{2+} and Ba^{2+}.

drastic swelling behavior is observed. This response resembles that observed in solutions of chaotropic anions to a lesser extent. In contrast, the minor swelling of the PCysMA brushes in the presence of barium cations is independent of concentration.

Ellipsometry provides useful information about the structure of PCysMA brushes in the presence of divalent cations. However, ATR-FTIR has proved to be even more powerful at understanding the physical networks formed by divalent metal-ion-containing polymer brushes.[38] Metal ions can coordinate via carboxylate coordination, i.e., monodentate, bridging bidentate, and chelating bidentate coordinations.[38,44] Therefore, the response of the PCysMA brushes in the presence of Ca^{2+} and Ba^{2+} ions at various concentrations was measured through ATR-FTIR, and the resulting spectra are shown in Figures 6 and S7. At very low concentration of 10^{-6} M, only

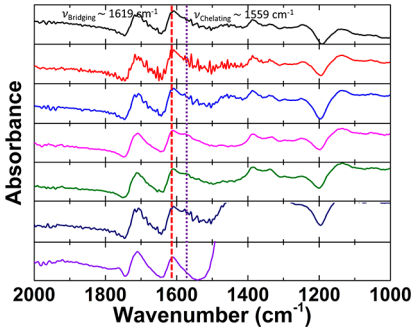

Figure 6. ATR-FTIR spectra of PCysMA brushes in 10^{-6}, 10^{-5}, 10^{-4}, 10^{-3}, 10^{-2}, 10^{-1}, and 1 M $Ca(NO_3)_2$ solutions (from top to bottom).

the asymmetric stretch vibration of carboxylate groups appeared at 1619 cm^{-1}, indicating that the coordination between cations and carboxylate moieties was dominated by bridging bidentate. With increasing salt concentration, a shoulder positioned at 1559 cm^{-1} started to emerge, corresponding to the chelating bidentate complexes. Surprisingly, the shoulder disappeared when the sample was exposed to a concentration of 1 M. While the shoulder height roughly increased with increasing $Ca(NO_3)_2$ concentration, due to the low signal nature of the brushes on silicon substrates for ATR-FTIR measurements, quantitative analysis could lead to erroneous conclusions. The changes observed with ATR-FTIR may be correlated to the complex species present at various concentrations. At low Ca^{2+} concentrations, each calcium ion can coordinate with as many carboxylate groups as possible. In this scenario, a more compact bridging bidentate complex was formed. At intermediate concentrations, as more carboxylate groups participate in the coordination with Ca^{2+}, a combination of bridging and chelating bidentate complexes was adopted. At high concentrations of $Ca(NO_3)_2$, calcium ions existed in surplus, and thus a monodentate structure would accommodate more calcium ions per carboxylate group. Under these conditions, the physical networks formed by divalent metal ion containing PCysMA brush were modulated by an ion screening effect, causing the brushes to swell as observed in ellipsometry experiments. In the series of $Ba(NO_3)_2$, the ATR-FTIR measurements were limited to 0.01 M due to salt precipitation problems. As carboxylate groups were in excess at 0.01 M, a similar phenomenon as in 0.01 M $Ca(NO_3)_2$ was seen.

The AFM height images revealed again smooth brush/solution interfaces in both $Ca(NO_3)_2$ (1 M) and $Ba(NO_3)_2$ (0.1 M) solutions, with a root-mean-square average of height deviation of 2.95 and 2.05 nm, respectively (Figures 7a and 7b). These values were close to those obtained in Milli-Q water, eliminating possible lateral structural heterogeneities of PCysMA brushes in divalent cationic solutions. With all the characterization methods combined, a deeper insight into the effect of divalent cations on the structure of PCysMA brushes can be achieved, as concluded in Scheme 2.

Effect of Trivalent Cation. Parallel to the studies performed with the divalent cations, the effect of trivalent cations on the brush structure was investigated using ellipsometry, as shown in Figure 8. The dimensions of the brush in $Y(NO_3)_3$ solution were similar to those in Milli-Q water up to a concentration of 3×10^{-3} M. Further increasing the concentration resulted in a collapse of the brush structure, which stands in direct opposition to the "antipolyelectrolyte" effect seen with mono- and divalent salt solutions. However, further increase of $Y(NO_3)_3$ concentration led to not only the

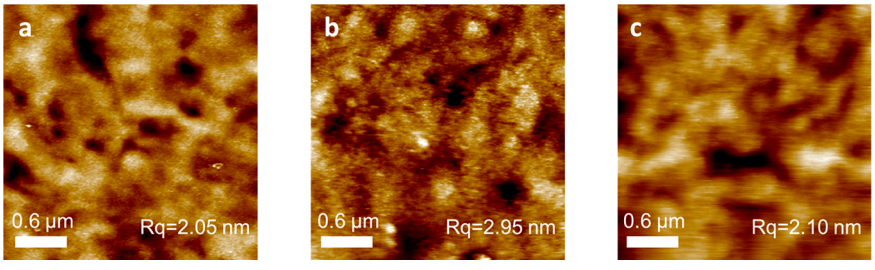

Figure 7. AFM height images of PCysMA brush in (a) 1 M $Ca(NO_3)_2$, (b) 0.1 M $Ba(NO_3)_2$, and (c) 1 M $Y(NO_3)_3$ solutions. Scan size: 3 μm × 3 μm (scale bars: 0.6 μm).

https://doi.org/10.1021/acs.macromol.2c02029
Macromolecules 2023, 56, 1945−1953

Scheme 2. Through Increasing the External Salt Concentration of $Ca(NO_3)_2$ or $Y(NO_3)_3$, a Zwitterionic Brush Can Chelate Multivalent Cations through Bridging Bidentate (a) to Bridging/Chelating Bidentate (b) and to Monodentate (c)

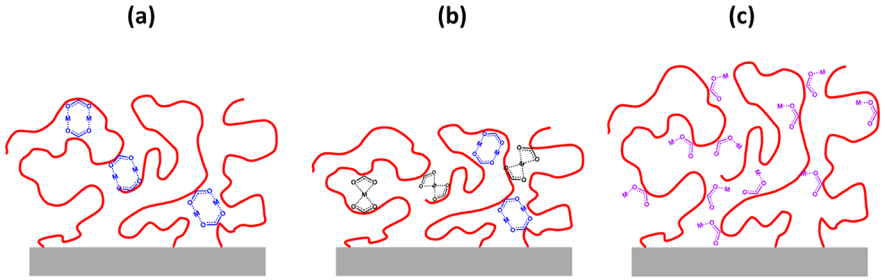

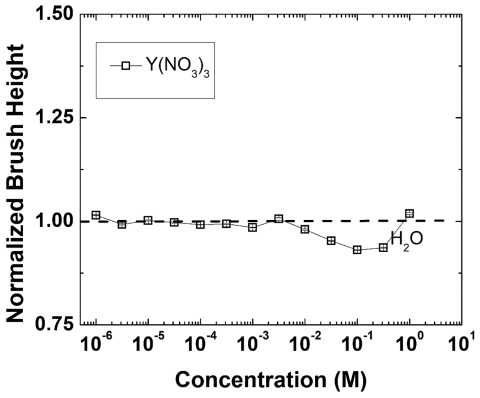

Figure 8. Brush height measured by ellipsometry plotted against the concentration of a trivalent cation, Y^{3+}.

recovery in brush dimension but also a subtle swelling of the brush structure. The range of concentration for which there is brush collapse can be attributed to the physical networks forming inside the brush layer due to the superior coordination capacity of Y^{3+}, which has been shown to produce a dramatic effect on PSS brush collapse in 10^{-5} M $Y(NO_3)_3$.[18,45] Of more interest was the dimensions recovery range, and to explore the underlying mechanism, ATR-FTIR was employed.

The ATR-FTIR spectra of PCysMA brush in $Y(NO_3)_3$ solutions are shown in Figure 9. For concentration values

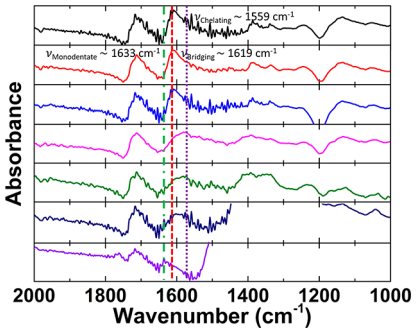

Figure 9. ATR-FTIR spectra of PCysMA brushes in 10^{-6}, 10^{-5}, 10^{-4}, 10^{-3}, 10^{-2}, 10^{-1}, and 1 M $Y(NO_3)_3$ solutions (from top to bottom).

between 10^{-6} and 10^{-4} M, the spectra showed almost identical features, and the peak of the signature asymmetric stretch vibration of carboxylate groups at 1619 cm^{-1} was always present, indicating the existence of coordination between cations and carboxylate moieties by a bridging bidentate complexing behavior.[38,44] Upon increasing the concentration, a dramatic broadening and change in the position of the carboxylate peak was observed, shifting to 1559 cm^{-1}. The broad peak distribution is due to different carboxylate vibration modes, revealing that both bridging and chelating bidentate complexes existed, with a higher population of chelating bidentate complexes in the system. As Y^{3+} possesses a higher coordination number than Ca^{2+} and Ba^{2+}, a more compact brush structure is required to accommodate these and results in a collapse of the dimensions of the PCysMA brushes as observed by ellipsometry. At the high concentration of 1 M, the peak shifted back to ca. 1633 cm^{-1}, which was similar to what was seen in Ca^{2+} solutions. The shift manifested a loosely monodentate complex structure forming between Y^{3+} and carboxylate groups in 1 M solution, and charge screening among polymer chains facilitated recovery in the brush dimension.

The results from the ellipsometry and ATR-FTIR experiments suggest it is of interest to investigate the lateral structural uniformity of the PCysMA brushes in trivalent cations. According to Ruths and co-workers, structural inhomogeneities occurred when the PSS brushes were immersed in $Y(NO_3)_3$ solutions.[45] To address this question, PCysMA brushes were measured with AFM, performed in a 1 M $Y(NO_3)_3$ solution (Figure 7c). In contrast to the phase separation observed in PSS brushes in a 0.1 mM $Y(NO_3)_3$ solution, a homogeneous lateral brush/solution interface was encountered, with an Rq value of 0.21 nm. In the case of PSS brushes, phase separation is attributed to the synergistic work of solvophobic and multivalent ion-induced effects.[45] Unexpectedly, in the case of PCysMA brushes, although multivalent ion-induced effects still exist, the much more solvophilic backbone of PCysMA prevents the ion−brush complexes from phase separating.

CONCLUSION

The structure of densely tethered PCysMA brushes generated via SI-ARGET-ATRP was systematically investigated to study the effects of monovalent, divalent, and trivalent ions. The results of ellipsometry, XRR, ATR-FTIR, and AFM measurements showed that zwitterionic PCysMA brushes exhibit an "antipolyelectrolyte" effect that follows the inverse Hofmeister series of anions in order of increasing chaotropicity. On the other hand, the brush dimension was altered in a less pronounced way by divalent cations such as Ca^{2+} and Ba^{2+}, while a collapsed structure was observed in the presence of trivalent Y^{3+} cations. These findings demonstrate that the structure of zwitterionic brushes can be manipulated by ionic species, highlighting the importance of ion specificity in the design of zwitterionic materials for a wide range of applications, including colloidal systems, responsive smart materials, and antifouling purposes.

https://doi.org/10.1021/acs.macromol.2c02029
Macromolecules 2023, 56, 1945−1953

■ ASSOCIATED CONTENT

Supporting Information

The Supporting Information is available free of charge at https://pubs.acs.org/doi/10.1021/acs.macromol.2c02029.

Table of SLD values for aqueous solutions; table of pH values for aqueous solutions; XRR spectra and fitting of dry and PCysMA brushes in the presence of water, NaSCN, NaBr, $NaNO_3$, NaCl, and Na_2SO_4 solutions, and corresponding scattering length densities (SLDs) of the PCysMA brush obtained from the best fittings of the XRR data presented; ATR-FTIR spectra of PCysMA brushes in D_2O, NaSCN, NaBr, $NaNO_3$, NaCl, Na_2SO_4, and $Ba(NO_3)_2$ solutions (PDF)

■ AUTHOR INFORMATION

Corresponding Authors

Qiming He − *Materials Science Division and Center for Molecular Engineering, Argonne National Laboratory, Lemont, Illinois 60439, United States; Pritzker School of Molecular Engineering, University of Chicago, Chicago, Illinois 60637, United States;* orcid.org/0000-0002-2652-3200; Email: qiminghe@uchicago.edu

Wei Chen − *Materials Science Division and Center for Molecular Engineering, Argonne National Laboratory, Lemont, Illinois 60439, United States; Pritzker School of Molecular Engineering, University of Chicago, Chicago, Illinois 60637, United States*; Email: wchen@anl.gov

Matthew V. Tirrell − *Materials Science Division and Center for Molecular Engineering, Argonne National Laboratory, Lemont, Illinois 60439, United States; Pritzker School of Molecular Engineering, University of Chicago, Chicago, Illinois 60637, United States;* orcid.org/0000-0001-6185-119X; Email: mtirrell@anl.gov

Authors

Yijun Qiao − *Materials Science Division and Center for Molecular Engineering, Argonne National Laboratory, Lemont, Illinois 60439, United States*

Carlos Medina Jimenez − *Pritzker School of Molecular Engineering, University of Chicago, Chicago, Illinois 60637, United States*

Ryan Hackler − *Chemical Sciences and Engineering Division, Argonne National Laboratory, Lemont, Illinois 60439, United States*

Alex B. F. Martinson − *Materials Science Division and Center for Molecular Engineering, Argonne National Laboratory, Lemont, Illinois 60439, United States;* orcid.org/0000-0003-3916-1672

Complete contact information is available at: https://pubs.acs.org/10.1021/acs.macromol.2c02029

Notes

The authors declare no competing financial interest.

■ ACKNOWLEDGMENTS

This work was supported by the Deaprtment of Energy, Basic Energy Sciences, Division of Materials Science and Engineering. C.M.J. was supported by the Department of Energy, Basic Energy Sciences, Critical Minerals & Materials Program Grant # DE-SC0022231. This research used resources of the Advanced Photon Source, a U.S. Department of Energy (DOE) Office of Science User Facilities operated for the DOE Office of Science by Argonne National Laboratory under Contract DE-AC02-06CH11357. In addition, we gratefully acknowledge the computing resources provided on Bebop, a high-performance computing cluster operated by the Laboratory Computing Resource Center at Argonne National Laboratory.

■ REFERENCES

(1) Jiang, S.; Cao, Z. Ultralow-Fouling, Functionalizable, and Hydrolyzable Zwitterionic Materials and Their Derivatives for Biological Applications. *Adv. Mater.* **2010**, *22* (9), 920−932.

(2) Shao, Q.; Jiang, S. Molecular Understanding and Design of Zwitterionic Materials. *Adv. Mater.* **2015**, *27* (1), 15−26.

(3) Hess, M.; Jones, R. G.; Kahovec, J.; Kitayama, T.; Kratochvíl, P.; Kubisa, P.; Mormann, W.; Stepto, R. F. T.; Tabak, D.; Vohlídal, J.; Wilks, E. S. Terminology of Polymers Containing Ionizable or Ionic Groups and of Polymers Containing Ions. *Pure Appl. Chem.* **2006**, *78* (11), 2067−2074.

(4) Kumar, R.; Fredrickson, G. H. Theory of Polyzwitterion Conformations. *J. Chem. Phys.* **2009**, *131* (10), 104901.

(5) Chen, S.; Zheng, J.; Li, L.; Jiang, S. Strong Resistance of Phosphorylcholine Self-Assembled Monolayers to Protein Adsorption: Insights into Nonfouling Properties of Zwitterionic Materials. *J. Am. Chem. Soc.* **2005**, *127* (41), 14473−14478.

(6) Higaki, Y.; Kobayashi, M.; Takahara, A. Hydration State Variation of Polyzwitterion Brushes through Interplay with Ions. *Langmuir* **2020**, *36* (31), 9015−9024.

(7) Schlenoff, J. B. Zwitteration: Coating Surfaces with Zwitterionic Functionality to Reduce Nonspecific Adsorption. *Langmuir* **2014**, *30* (32), 9625−9636.

(8) Erfani, A.; Seaberg, J.; Aichele, C. P.; Ramsey, J. D. Interactions between Biomolecules and Zwitterionic Moieties: A Review. *Biomacromolecules* **2020**, *21* (7), 2557−2573.

(9) Zhang, Z.; Chao, T.; Chen, S.; Jiang, S. Superlow Fouling Sulfobetaine and Carboxybetaine Polymers on Glass Slides. *Langmuir* **2006**, *22* (24), 10072−10077.

(10) Higaki, Y.; Kobayashi, M.; Murakami, D.; Takahara, A. Anti-Fouling Behavior of Polymer Brush Immobilized Surfaces. *Polym. J.* **2016**, *48* (4), 325−331.

(11) Baggerman, J.; Smulders, M. M. J.; Zuilhof, H. Romantic Surfaces: A Systematic Overview of Stable, Biospecific, and Antifouling Zwitterionic Surfaces. *Langmuir* **2019**, *35* (5), 1072−1084.

(12) *Poly(Ethylene Glycol) Chemistry: Biotechnical and Biomedical Applications*; Milton, H. J., Ed.; Plenum Press: New York, 1992.

(13) Ostuni, E.; Chapman, R. G.; Holmlin, R. E.; Takayama, S.; Whitesides, G. M. A Survey of Structure−Property Relationships of Surfaces That Resist the Adsorption of Protein. *Langmuir* **2001**, *17* (18), 5605−5620.

(14) Li, L.; Chen, S.; Zheng, J.; Ratner, B. D.; Jiang, S. Protein Adsorption on Oligo(Ethylene Glycol)-Terminated Alkanethiolate Self-Assembled Monolayers: The Molecular Basis for Nonfouling Behavior. *J. Phys. Chem. B* **2005**, *109* (7), 2934−2941.

(15) Zheng, J.; Li, L.; Tsao, H.-K.; Sheng, Y.-J.; Chen, S.; Jiang, S. Strong Repulsive Forces between Protein and Oligo (Ethylene Glycol) Self-Assembled Monolayers: A Molecular Simulation Study. *Biophys. J.* **2005**, *89* (1), 158−166.

(16) He, Y.; Chang, Y.; Hower, J. C.; Zheng, J.; Chen, S.; Jiang, S. Origin of Repulsive Force and Structure/Dynamics of Interfacial Water in OEG−Protein Interactions: A Molecular Simulation Study. *Phys. Chem. Chem. Phys.* **2008**, *10* (36), 5539.

(17) Feng, W.; Brash, J.; Zhu, S. Non-Biofouling Materials Prepared by Atom Transfer Radical Polymerization Grafting of 2-Methacryloloxyethyl Phosphorylcholine: Separate Effects of Graft Density and Chain Length on Protein Repulsion. *Biomaterials* **2006**, *27* (6), 847−855.

(18) Yu, J.; Mao, J.; Yuan, G.; Satija, S.; Jiang, Z.; Chen, W.; Tirrell, M. Structure of Polyelectrolyte Brushes in the Presence of Multivalent Counterions. *Macromolecules* **2016**, *49* (15), 5609−5617.
(19) Alswieleh, A. M.; Cheng, N.; Canton, I.; Ustbas, B.; Xue, X.; Ladmiral, V.; Xia, S.; Ducker, R. E.; El Zubir, O.; Cartron, M. L.; Hunter, C. N.; Leggett, G. J.; Armes, S. P. Zwitterionic Poly(Amino Acid Methacrylate) Brushes. *J. Am. Chem. Soc.* **2014**, *136* (26), 9404−9413.
(20) Kang, B.; Tang, H.; Zhao, Z.; Song, S. Hofmeister Series: Insights of Ion Specificity from Amphiphilic Assembly and Interface Property. *ACS Omega* **2020**, *5* (12), 6229−6239.
(21) Marcus, Y. Effect of Ions on the Structure of Water: Structure Making and Breaking. *Chem. Rev.* **2009**, *109* (3), 1346−1370.
(22) Jakubowski, W.; Min, K.; Matyjaszewski, K. Activators Regenerated by Electron Transfer for Atom Transfer Radical Polymerization of Styrene. *Macromolecules* **2006**, *39* (1), 39−45.
(23) Tolan, M.; Ward, M. D. X-Ray Scattering from Soft-Matter Thin Films: Materials Science and Basic Research. *Phys. Today* **2000**, *53* (1), 58−58.
(24) Ladmiral, V.; Charlot, A.; Semsarilar, M.; Armes, S. P. Synthesis and Characterization of Poly(Amino Acid Methacrylate)-Stabilized Diblock Copolymer Nano-Objects. *Polym. Chem.* **2015**, *6* (10), 1805−1816.
(25) Dewick, P. M. *Essentials of Organic Chemistry: For Students of Pharmacy, Medicinal Chemistry and Biological Chemistry*; Wiley-VCH: 2006.
(26) Delgado, J. D.; Schlenoff, J. B. Static and Dynamic Solution Behavior of a Polyzwitterion Using a Hofmeister Salt Series. *Macromolecules* **2017**, *50* (11), 4454−4464.
(27) Lee, H.; Pietrasik, J.; Sheiko, S. S.; Matyjaszewski, K. Stimuli-Responsive Molecular Brushes. *Prog. Polym. Sci.* **2010**, *35* (1−2), 24−44.
(28) Murdoch, T. J.; Willott, J. D.; de Vos, W. M.; Nelson, A.; Prescott, S. W.; Wanless, E. J.; Webber, G. B. Influence of Anion Hydrophilicity on the Conformation of a Hydrophobic Weak Polyelectrolyte Brush. *Macromolecules* **2016**, *49* (24), 9605−9617.
(29) Deodhar, C.; Soto-Cantu, E.; Uhrig, D.; Bonnesen, P.; Lokitz, B. S.; Ankner, J. F.; Kilbey, S. M. Hydration in Weak Polyelectrolyte Brushes. *ACS Macro Lett.* **2013**, *2* (5), 398−402.
(30) Murdoch, T. J.; Humphreys, B. A.; Willott, J. D.; Gregory, K. P.; Prescott, S. W.; Nelson, A.; Wanless, E. J.; Webber, G. B. Specific Anion Effects on the Internal Structure of a Poly(N-Isopropylacrylamide) Brush. *Macromolecules* **2016**, *49* (16), 6050−6060.
(31) Sakamaki, T.; Inutsuka, Y.; Igata, K.; Higaki, K.; Yamada, N. L.; Higaki, Y.; Takahara, A. Ion-Specific Hydration States of Zwitterionic Poly(Sulfobetaine Methacrylate) Brushes in Aqueous Solutions. *Langmuir* **2019**, *35* (5), 1583−1589.
(32) Higaki, Y.; Inutsuka, Y.; Sakamaki, T.; Terayama, Y.; Takenaka, A.; Higaki, K.; Yamada, N. L.; Moriwaki, T.; Ikemoto, Y.; Takahara, A. Effect of Charged Group Spacer Length on Hydration State in Zwitterionic Poly(Sulfobetaine) Brushes. *Langmuir* **2017**, *33* (34), 8404−8412.
(33) Kobayashi, M.; Ishihara, K.; Takahara, A. Neutron Reflectivity Study of the Swollen Structure of Polyzwitterion and Polyeletrolyte Brushes in Aqueous Solution. *J. Biomater. Sci. Polym. Ed.* **2014**, *25* (14−15), 1673−1686.
(34) Galvin, C. J.; Dimitriou, M. D.; Satija, S. K.; Genzer, J. Swelling of Polyelectrolyte and Polyzwitterion Brushes by Humid Vapors. *J. Am. Chem. Soc.* **2014**, *136* (36), 12737−12745.
(35) Dunlop, I. E.; Thomas, R. K.; Titmus, S.; Osborne, V.; Edmondson, S.; Huck, W. T. S.; Klein, J. Structure and Collapse of a Surface-Grown Strong Polyelectrolyte Brush on Sapphire. *Langmuir* **2012**, *28* (6), 3187−3193.
(36) Mason, P. E.; Neilson, G. W.; Dempsey, C. E.; Barnes, A. C.; Cruickshank, J. M. The Hydration Structure of Guanidinium and Thiocyanate Ions: Implications for Protein Stability in Aqueous Solution. *Proc. Natl. Acad. Sci. U. S. A.* **2003**, *100* (8), 4557−4561.
(37) Aulich, D.; Hoy, O.; Luzinov, I.; Brücher, M.; Hergenröder, R.; Bittrich, E.; Eichhorn, K.-J.; Uhlmann, P.; Stamm, M.; Esser, N.; Hinrichs, K. In Situ Studies on the Switching Behavior of Ultrathin Poly(Acrylic Acid) Polyelectrolyte Brushes in Different Aqueous Environments. *Langmuir* **2010**, *26* (15), 12926−12932.
(38) Dehghani, E. S.; Naik, V. V.; Mandal, J.; Spencer, N. D.; Benetti, E. M. Physical Networks of Metal-Ion-Containing Polymer Brushes Show Fully Tunable Swelling, Nanomechanical and Nanotribological Properties. *Macromolecules* **2017**, *50* (6), 2495−2503.
(39) Hayashi, S.; Adachi, K.; Tezuka, Y. An Efficient Route to Cyclic Polymers by ATRP−RCM Process. *Chem. Lett.* **2007**, *36* (8), 982−983.
(40) Barth, A. Infrared Spectroscopy of Proteins. *Biochim. Biophys. Acta - Bioenerg.* **2007**, *1767* (9), 1073−1101.
(41) Onsager, L. Electric Moments of Molecules in Liquids. *J. Am. Chem. Soc.* **1936**, *58* (8), 1486−1493.
(42) Collins, K. D.; Washabaugh, M. W. The Hofmeister Effect and the Behaviour of Water at Interfaces. *Q. Rev. Biophys.* **1985**, *18* (4), 323−422.
(43) Vlachy, N.; Jagoda-Cwiklik, B.; Vácha, R.; Touraud, D.; Jungwirth, P.; Kunz, W. Hofmeister Series and Specific Interactions of Charged Headgroups with Aqueous Ions. *Adv. Colloid Interface Sci.* **2009**, *146* (1−2), 42−47.
(44) Deacon, G. Relationships between the Carbon-Oxygen Stretching Frequencies of Carboxylato Complexes and the Type of Carboxylate Coordination. *Coord. Chem. Rev.* **1980**, *33* (3), 227−250.
(45) Yu, J.; Jackson, N. E.; Xu, X.; Brettmann, B. K.; Ruths, M.; de Pablo, J. J.; Tirrell, M. Multivalent Ions Induce Lateral Structural Inhomogeneities in Polyelectrolyte Brushes. *Sci. Adv.* **2017**, *3* (12), eaao1497.

https://doi.org/10.1021/acs.macromol.2c02029
Macromolecules 2023, 56, 1945−1953